C-band Dual-polarimetric Radar Signatures of Hail

MATTHEW E. ANDERSON[+*], LAWRENCE D. CAREY[+**], WALTER A. PETERSEN[^], and KEVIN R. KNUPP[+]
[+]University of Alabama in Huntsville (UAHuntsville), Huntsville, Alabama
[^]NASA Marshall Space Flight Center (MSFC), Huntsville, Alabama

(Manuscript received 14 January 2011; in final form 21 April 2011)

ABSTRACT

Many studies have demonstrated that dual-polarimetric radar is an effective tool for hail detection. Studies employing radar at S-band frequencies have typically found that hail is characterized by high reflectivity (Z_h > 50 dBZ) and near zero differential reflectivity (-1 < Z_{dr} < 1 dB) at and just above the ground. Several studies have hypothesized that hail signatures observed by higher frequency radars, such as C-band, should be similar. To test the hypothesis, the dual-polarimetric radar signatures of nine hail events, including 46 hail producing convective cells and 172 hail reports, are carefully documented using C-band radar observations over the Alabama and Tennessee border region. Unlike prior results at S-band, this study shows that hail at C-band is typically characterized by high Z_h (> 50 dBZ) and high Z_{dr} (3 – 8 dB) at and just above the ground.

1. Introduction

Severe storms are important to identify and forecast because of the significant damage and fatalities that they can cause. A severe thunderstorm is defined by the National Weather Service (NWS) as a storm that produces large hail (diameter ≥ 1.9 cm at the start of this study), strong winds (> 26 m/s), or a tornado. During the course of this study, the NWS definition of severe hail changed to a hail diameter ≥ 2.5 cm [1]. One large hail producing storm can cause 100's of millions of dollars of property damage to crops, livestock, homes, and automobiles (Hillaker et al. 1985, Changnon 1999). Large hail, in rare cases, can even cause bodily injury or death to people and livestock (Ludlam 1980, Appendix 8.12; National Climate Data Center

[1] National Weather Service Instruction (NWSI) 10-511, April, 19, 2010: http://www.nws.noaa.gov/directives/

*Current Affiliation: National Weather Service, Topeka, Kansas.
**Corresponding author address: Dr. Larry Carey, 320 Sparkman Dr, Huntsville, AL 35805
E-mail: larry.carey@nsstc.uah.edu

(NCDC)). Clearly, it is important to identify areas of hail so that lives and property can be protected. To this end, ground-based radar is the most widely utilized observational tool for detecting and nowcasting hail (e.g. Greene and Clark 1972, Eccles and Atlas 1973, Mather et al. 1976, Bringi et al. 1984, Edwards and Thompson 1998).

Dual-polarization radar observations have improved the ability of the radar meteorologist to identify hydrometeor type, including hail. Studies for the classification of hydrometeors based on their polarimetric variables have been conducted at both S-Band (e.g. Aydin et al. 1986, Bringi et al. 1986, Hubbert et al. 1998, Straka et. al. 2000), C-Band (e.g. Meischner et al. 1991, Höller et al. 1994, Keenan et al. 2003, Deierling et al. 2005, Tabary et al. 2009a, Tabary et al. 2010) and X-band (e.g. Dolan and Rutledge 2009, Snyder et al. 2010) wavelengths. The use of C-band dual-polarimetric radars is becoming more common among worldwide operational weather services, including Australia and many Asian and European countries, the private market (e.g. media broadcasting) for forecasting in the United States, and worldwide universities for research purposes due to their affordability. As a result, it is important to document carefully the C-band dual-polarimetric radar signatures of hail. This study examines the polarimetric radar signatures of 46 well sampled, hail producing convective cells on nine different days over the Alabama and Tennessee border region using the UAHuntsville-NASA Advanced Radar for Meteorological and Operational Research (ARMOR) (Petersen et al. 2007).

2. Previous dual-polarimetric radar hail studies

There are numerous literature examples demonstrating the effectiveness of hail identification using dual-polarimetric radar variables. For example, differential reflectivity (Z_{dr})

is a measure of the decibel reflectivity difference between horizontal (Z_h) and vertical (Z_v) polarizations (Bringi and Chandrasekar 2001 p. 381). Therefore, Z_{dr} is helpful in estimating the oblateness of a hydrometeor. The more oblate the particle the larger Z_{dr} is. In rain, Z_{dr} is positive (typical values of 1 to 4 dB) and steadily increases with Z_h (Bringi and Chandrasekar 2001 p. 397). For large Z_h (> 50 dBZ), Z_{dr} is typically > 2.5 dB in rain. Hailstones are typically less oblate than raindrops and therefore are associated with lower Z_{dr}. The effect of oblateness on Z_{dr} in hail can be further reduced relative to rain because of the random orientations associated with tumbling and a lower dielectric constant for hail (Straka et al. 2000). As a result, hail can appear to the radar as an "effective sphere" and Z_{dr} is typically near 0 dB. Several S-band dual polarimetric radar-based studies have found hail to be characterized by near zero Z_{dr} ($|Z_{dr}| < 1$ dB) and large Z_h (> 50 dBZ) near the surface (Bringi et al. 1984, Illingworth et al. 1986, Bringi et al. 1986, Aydin et al. 1990, Herzegh and Jameson 1992, Hubbert et al. 1998). The dual-polarimetric radar-based hail signature of a minimum in Z_{dr} has been termed the "Z_{dr}-hole" (Wakimoto and Bringi 1988) because of the low Z_{dr} (hail) region surrounded by a higher Z_{dr} (rain) area in a region of large Z_h (Fig. 1) (Bringi et al. 1986, Bringi and Chandrasekar 2001, p. 451-456). Other radar studies at S-band have shown that Z_{dr} associated with melting hail can be moderately positive ($0 < Z_{dr} < 2.5$ dB) but is typically smaller than in rain for a given Z_h (Leitao and Watson 1984, Aydin et al. 1986, Straka et al. 2000, Heinselman and Ryzhkov 2006, Depue et al. 2007). This anti-correlation between large Z_h and relatively small Z_{dr} forms the basis of most S-band dual-polarimetric radar hail detection algorithms. Several authors suggest that these methods to detect large hail can be directly applied at C-band (e.g. Vivekanandan et al. 1990, Aydin and Giridhar and 1992, Bringi and Chandrasekar 2001 p 451-452).

The correlation coefficient (ρ_{hv}) is the co-polar correlation of the pulse to pulse returns between the horizontal and vertical polarizations in a given radar volume. In a radar volume that contains rain, ρ_{hv} is expected to be high, greater than 0.98 at S-band and 0.95 at C-band (e.g. Bringi et al. 1991, Carey et al. 2000, Keenan et al. 2000). The suppressed values of ρ_{hv} (0.95 to 0.98) in rain at C-band are associated with large drops that produce resonant scattering. Values of ρ_{hv} for hail at S-band (Balakrishnan and Zrnic 1990) and C-band (Tabary et al. 2010) have been found to be below 0.95. Low (< 0.95) ρ_{hv} in regions of hail and melting hail can be explained by non-Rayleigh (Mie or resonant) scattering, irregular shaped hydrometeors, mixture of hydrometeors (e.g. rain and melting hail), and a variety of hydrometeor shapes, dielectric constants and fall modes (Balakrishnan and Zrnic 1990).

At C-band frequency, Meischner et al. (1991), Ryzhkov et al. (2007), Tabary et al (2009a) and Tabary et al. (2010) have shown that near 0 dB or even low (< 2.5 dB) Z_{dr} is not necessarily what can be expected in areas of melting hail (Fig. 2). Meischner et al. (1991) attributes the anomalously high Z_{dr} (> 5 dB) to smaller melting hail and resonance effects due to the smaller wavelength. Smaller melting hailstones can appear to the radar as large wet raindrops and exhibit high Z_{dr}. Resonance begins to take place at C-Band for rain and melting hailstones larger than about 5 mm (Zrnic et al. 2000). Therefore, when large particles are present Z_{dr} can be significantly higher at C-Band compared to S-Band (Zrnic et al. 2000). Ryzhkov et al. (2007) suggest that the anomalously high Z_{dr} can be explained by large raindrops and small melting hail that dominate Z_h in melting hail shafts. Tabary et al. (2009a) and Tabary et al. (2010) demonstrate that confirmed cases of melting hail and rain and hail mixtures are typically associated with Z_{dr} > 3 dB and as high as 8 dB or more. All of the above C-band studies indicate that the S-band approach for hail identification of high Z_h and low Z_{dr} may not always work at C-

band. On the other hand, Bringi and Chandrasekar (2001) (p.451-452) and Ryzhkov et al. (2009) suggest that the Z_{dr}-hole ($|Z_{dr}| < 1.0$ dB and large $Z_h > 50$ dBZ) should be observed at C-band when hailstones are large and numerous enough to dominate Z_h and appear as effective spheres. Using a radar model of melting hailstones, Vivekanandan et al. (1990) suggest that hail above 12-15 mm in diameter shed their melt water and tumble, leading to the "Z_{dr}-hole" signature at C-band. Clearly, dual-polarimetric radar signatures of hail at C-band must be better understood in order to properly identify hail and provide warning of severe storms.

3. Data and Methodology

The radar used for this study is the UAHuntsville-NASA ARMOR C-band dual-polarimetric radar, which is located at the Huntsville International Airport. Further specifications for ARMOR can be found in Petersen et al. (2007). For all but two events (May 20, 2008 and August 2, 2008), the ARMOR is in a PPI sector volume scanning mode, which includes multiple scanning elevation angles between user selected azimuths and is used to sample select storms well in the horizontal and vertical every 2 to 3 minutes. The other scanning method is a routinely used operational series of full 360° surveillance scans at the lowest three elevation angles (0.7°, 1.3°, and 2.0°) that repeat every 3 to 5 minutes. ARMOR Z_h and Z_{dr} are the primary variables used to characterize hail in this study. ARMOR ρ_{hv} is used to identify potential areas of rain-hail mixtures associated with melting hail. At C-band, a mixture of partially melted hail and large rain drops originating from melting hail should be characterized by low ρ_{hv} (< 0.95) because of resonant scattering and a variety of hydrometeor shapes, dielectric constants and fall modes in the radar resolution volume (Balakrishnan and Zrnic 1990,

Meischner et al. 1991, Tabary et al. 2010). Z_{dr} has been calibrated using vertically pointing scans in light rain (Gorgucci et al. 1999). Z_h has been calibrated using self-consistency among dual-polarimetric variables (Ryzhkov et al. 2005).

Z_h and Z_{dr} have been corrected for attenuation and differential attenuation, respectively, using the differential phase (Bringi et al. 2001). ARMOR is run for operational purposes across the Tennessee Valley and the data has been shown effective in other studies (e.g. Deierling et al. 2005, Gatlin et al. 2009). Recently, attempts have been made to develop and use improved propagation correction methods that account for "hot spots" associated with regions of resonant-sized large rain drops and/or melting hailstones that cause enhanced attenuation and differential attenuation at C-band (Carey et al. 2000, Tabary et al. 2009b, Gu et al. 2011). Although promising, these recent methods have not yet been widely tested for their usefulness with operational objectives and are therefore not utilized herein.

In order to investigate the C-band polarimetric signatures of hail, ARMOR data and storm reports are used from 9 different hail events, including 46 convective cells and 172 hail reports (Table 1). Hail report sizes range from 0.6 cm to 10.8 cm and average about 3.3 cm. The overwhelming majority of hailstone reports have sizes$\geq$ 1.9 cm, which met the NWS definition of severe during most of this study, while 65% of the reports (111) meet the current NWS definition of severe hail. The locations, magnitudes, and timing of observed hail were obtained from the NCDC *Storm Data*. For the prolific hail producing event of April 10, 2009, an Internet survey of hail properties was also conducted among UAHuntsville and NASA staff and students. Each hail report was evaluated carefully for accuracy by comparing archived radar data to its time and location. If a 50 dBZ echo did not occur within +/- 15 minutes and 1 km of a hail report, then the report was not used in the study. The 1 km/15 minute criteria were used to

capture all potential hail data and to account for inaccuracies in the location and time of reports. Table 2 shows different environmental factors that affect the hailstone melting process such as the melting level, temperature lapse rate, relative humidity and the surface temperature. The data were obtained from archived RUC (Rapid Update Cycle) model soundings from the Huntsville, AL area.

Although plan position indicator (PPI) images of Z_h and Z_{dr} for all 46 hail producing convective cells were visually inspected for hail signatures (e.g., Fig. 3), the quantitative results in this study rely on characterizing Z_h and Z_{dr} within a 1 km radius of each quality controlled hail report. Analysis radii of 0.5 km and 1.5 km were also tested but had little effect on the overall results and are therefore not shown. Joint absolute frequency histogram plots of Z_{dr} versus Z_h at low levels (i.e., data below 1 km in height) and contoured frequency by altitude diagrams (CFADs) of Z_{dr} versus height (Yuter et al. 1995) are used to evaluate hail signatures at C-band for the April 10, 2009 event (5 cells, 77 hail reports). For the composite analysis of all nine hail events (46 cells, 172 hail reports), joint relative frequency histograms of Z_{dr} versus Z_h are created using low-level data (data below 1 km in height) in which the absolute count in each bin is divided by the total bin count and is expressed in percent. Similarly, CFADs of the Z_{dr} and ρ_{hv} versus height relative to the 0 °C level (H_0, km) were used to evaluate the signature of melting hail associated with the composite analysis. These diagrams are also made by dividing the absolute count in each bin by the total bin count and are expressed in percent. Histogram bin sizes used in this study are: 2 dBZ for Z_h, 0.5 dB for Z_{dr}, 0.01 for ρ_{hv}, and 250 m for height.

4. Results

We begin by presenting results from the prodigious hail producing event of April 10, 2009. Although not shown herein, the polarimetric signatures of the other hail events have been studied separately and are consistent with the results from April 10, 2009. To summarize the overall results of the study, we show composite statistical analyses of all nine hail events.

a. April 10, 2009 hail event

The PPI shows a storm in close proximity to the radar (10-15 km) crossing over highly populated areas where a large number of reports were received (Fig. 3). The first PPI (Fig. 3a) is taken from the lowest elevation scan of 0.7° and is a good representation of Z_h and Z_{dr} closest to the surface. The Z_h shows areas in the cell of high values (> 55 dBZ) associated with particles of large diameters possibly large raindrops, hail, and melting hail that fall into the resonance size region. It can be seen that high Z_h (> 50 dBZ) is associated with high Z_{dr} (3-8 dB) near the surface (Fig. 3a). In some radar gates, the corrected Z_{dr} is as high as 10 dB. There is no evidence of the "Z_{dr}-hole" that is typically found at S-band. The PPIs in Fig. 3b indicate a persistent, large area of enhanced Z_{dr} (3-8 dB) associated with high Z_h (> 50 dBZ) at heights of about 1.1 km above radar level (i.e., range ~ 15 km and elevation angle = 4.2°). Since the 0°C height level is at 3 km, it is hypothesized that melting of resonant sized hailstones and a mixture of hydrometeors is causing this high Z_{dr} (3-8 dB). The PPIs in Fig. 3c at 11° elevation angle show that higher in the storm (i.e., height > 3 km at range > 15 km) low Z_{dr} (-1 to 1 dB) is associated with high Z_h (> 50 dBZ). The low Z_{dr} is likely due to tumbling dry hail and graupel found above the 0° C height level.

The joint frequency histogram of Z_{dr} versus Z_h (Fig. 4) from the radar range gates located at heights below 1 km and within 1 km of the hail reports are characterized by anomalously high Z_{dr} for areas of high Z_h. There is a Z_{dr} mode of 5 dB that occurs at 54 dBZ. Maximum Z_{dr} values are observed as high as 10 dB (Fig. 4). For the Z_h bin from 55-57 dBZ, the 25th, 50th, and 75th percentiles of Z_{dr} are 4.0, 5.6, and 7.0 dB, respectively, with a mean of 5.4 dB. This indicates that 50 % of the Z_{dr} data within the 55 – 57 dBZ bin can be found between 4.0 and 7.0 dB. These results are similar to what was found in Meischner et al. (1991). However, the anomalously high Z_{dr} observed in Meischner et al. (1991) is hypothesized to be due to smaller melting hailstones that appear as large raindrops to the radar. When melting occurs, the water torus on the outside of the drop can become sufficient enough to stabilize the hailstone (Rasmussen and Heymsfield 1987). In this case, one would expect high Z_{dr}. Zrnic et al. (2000) notes that wet particles over 5 mm at C-band are in the resonant scattering regime and can cause peaks in Z_{dr} for particles greater than 5 mm. All reported hailstone diameters in this study are well over 5 mm, therefore, resonant scattering could be contributing to the anomalously high Z_{dr}. However, there is no certainty that only hail and melting hail are present in the data set and other hydrometeors, such as large raindrops, could have contributed to the signatures.

In addition to analyzing the Z_{dr} and Z_h polarimetric signatures, the hail signal H_{dr} developed by Aydin et al. (1986) for use at S-band was plotted (Fig. 4). Aydin and Giridhar (1992) suggest that this method can be applied to C-band with little modification. The solid red line in Fig. 4 is where H_{dr} is 0 dB. Areas to the right and below the line are where H_{dr} is positive and is taken to signify hail, while areas to the left and above the line are where H_{dr} is negative and is assumed to indicate rain (Aydin et al. 1986). It can be seen that just the opposite occurs in the C-band ARMOR observations. Most of the hail observations fall on the negative side of the

plot where rain is expected at S-band except for the points greater than 60 dBZ where Aydin et al. (1986) assumes data above this value are associated with hail. These results indicate that the conventional behavior of S-band Z_h and Z_{dr} does not apply at C-band for this hail event.

A striking result that also goes against traditional S-band knowledge can be found in the CFAD of Z_{dr} (Fig. 5). The 0 °C level indicated on the 17 UTC sounding from Redstone Arsenal, located 8 km to the east of the ARMOR C-band polarimetric radar, is around 3 km. Z_{dr} in this example is around 0 dB above the 0 °C level, which is what has also been observed at S-Band. As the hail continues below the 0 °C level, Z_{dr} begins to increase toward high positive values with a mode near the surface of 5.5 dB and a maximum of near 10 dB, which is unlike past S-band studies. For the height bin from 0 to 250 m, the 25th, 50th, and 75th percentiles of Z_{dr} are 4.0, 5.5, 6.9 dB, respectively, with mean of 5.5 dB while well above the 0 °C level at the 4.0 to 4.25 km bin the 25th, 50th, and 75th percentiles of Z_{dr} are -0.2, 0.1, and 0.5, respectively, with a mean of 0.2 dB. This indicates that near the surface (0 – 250 m) 50 % of the Z_{dr} data occurs between 4.0 and 6.9 dB while aloft (4.0 – 4.25 km) the distribution of data is narrower with the 50 % of data occurring between -0.2 and 0.5 dB. Therefore, near the surface resonant sized (> 5 mm at C-band), stably oriented and melting hailstones, possibly mixed with large raindrops, are likely enhancing Z_{dr}. The increase in Z_{dr} takes place below about 1.6 km where the hailstones have likely had enough time to begin melting and developing a sufficient water torus. Interestingly, the Z_{dr} distribution starts broadening, including more negative and positive values, at about 2 km before shifting to more distinctly positive values between 1.6 km and 1 km. Table 2 indicates mid-level average relative humidity for the April 10th event to be near 14 %. Rasmussen and Pruppacher (1982) indicate that atmospheres with lower RH's can delay the

onset of melting. This effect of low RH could be the reason why shifts in the Z_{dr} data for Fig. 5 are seen near 1 km below the 0 °C level.

b. Composite of all nine hail events

The joint relative frequency distribution of Z_{dr} versus Z_h reveals a high Z_{dr} mode of 5 dB with Z_h between 51 to 57 dBZ (Fig. 6). Figure 6 indicates the 25th, 50th, and 75th percentiles for the Z_h bin from 55 to 57 dBZ are 4.0, 5.5, and 6.9 dB, respectively, with a mean of 5.3 dB. Therefore, 50 % of the data in the 55 to 57 dBZ bin is in between 4.0 to 6.9 dB. In addition to the high Z_{dr} mode, an increase in Z_{dr} occurs as Z_h increases. The high Z_{dr} may be due to melting, stably oriented hailstones, possibly mixed with raindrops, which fall into the resonance regime at C-band (Meischner et al. 1991, Vivekanandan et al. 1990, Ryzhkov et al. 2007).

The CFAD of Z_{dr} indicates a clear shift in Z_{dr} from near 0 dB aloft (i.e., heights above 0 °C level) to large positive Z_{dr} values below the 0 °C level (H_0) with the dramatic increase in Z_{dr} beginning at H_0 = -1.5 km (Fig. 7). Figure 7 is similar to Fig. 5 due to the overwhelming majority of points from the April 10, 2009 event. For the H_0 bin from -2.50 to -2.25 km, the 25th, 50th, and 75th percentiles for Z_{dr} are 3.2, 5.2, and 6.9 dB, respectively, with a mean of 5.3 dB while above the 0 °C level from H_0 = 0.75 to 1.00 km bin the 25th, 50th, and 75th percentiles for Z_{dr} are -0.2, 0.1, and 0.5 dB, respectively, with a mean of 0.4 dB. Figure 7 suggests that significant microphysical changes, which are likely driven by the melting of hail, are occurring to cause the sudden increase in Z_{dr} near the surface. Figure 8 confirms this mixture below the freezing level by showing a dramatic shift in the ρ_{hv} data as well. For the H_0 bin from -2.50 to -2.25 km, the 25th, 50th, and 75th percentiles for ρ_{hv} are 0.88, 0.93, and 0.96, respectively, with a mean of 0.92 while above the 0 °C level from H_0 = 0.75 to 1.00 km bin the 25th, 50th, and 75th

percentiles for ρ_{hv} are 0.95, 0.98, and 0.99, respectively, with a mean of 0.96. Table 2 indicates a range of environmental factors that can contribute to melting hailstones. Mid-level relative humidity (RH) varies from 14 – 86 %. Rasmussen and Heymsfield (1987b) indicate that an atmosphere with higher RH's will experience melting first while hailstones falling in atmospheres with lower RH's will experience delayed melting closer to the surface. With the numerous hail reports from the April 10, 2009 event, this delayed melting associated with lower RH may be why the shift in the polarimetric signatures associated with melting are not observed until 1 km below the 0 °C height level (i.e., H_0 = -1 km). As seen in Table 2, the heights of the 0 °C level range from 2.64 to 4.81 km above ground level (AGL). These 0 °C heights should provide significant time for melting to occur with surface temperatures ranging from 14.1 - 30.9 °C. Lapse rates for the events studies range from 5.1 to 7.6 °C/km. Rasmussen and Heymsfield (1987b) noted that hailstones can melt more quickly in higher temperature lapse rates.

Overall, the April 10, 2009 and composite analysis of Z_{dr} versus Z_h and Z_{dr} versus height reveal similar results. In regions of hail and melting hail, near surface values of Z_{dr} are typically 3 to 8 dB while Z_{dr} values above the 0 °C height level, H_0, are typically -0.2 to 0.5 dB. The transition from near zero Z_{dr}, which is consistent with dry, tumbling hail, to large Z_{dr}, which is consistent with resonance sized melting hail likely mixed with large rain drops, begins to occur around 1 km below H_0 (H_0 = -1 km). Composite analysis of ρ_{hv} with H_0 reveals suppressed values of ρ_{hv} (< 0.95) increasing in frequency between H_0 = 0 km and H_0 = -1 km and being quite common for $H_0 \leq$ -1 km, supporting the idea that the melting of hail is actively occurring between H_0 = 0 km and H_0 = -1 km and that a mixture of resonance sized melting hail and large rain drops is likely present at H_0 < -1 km.

5. Summary and Conclusions

ARMOR observations show that the C-band dual-polarimetric radar-based signatures of large hail (average size of 3.3 cm) are typically characterized by high Z_h (> 50 dBZ), high Z_{dr} (3-8 dB), and low ρ_{hv} (< 0.95) at low-levels. Therefore, the hypothesis that C-band radar signatures of large hail are usually consistent with the S-band "Z_{dr}-hole" signature of high Z_h (> 50 dBZ) and low Z_{dr} (-1 to 1 dB) at low-levels has been rejected through careful observation of nine hail events, 46 convective cells and 172 hail reports, suggesting that S-band techniques for identifying large hail using Z_{dr} cannot be directly applied at C-band without modifications.

It is hypothesized in this study along with others (Vivekanandan et al. 1990, Meischner et al. 1991, Zrnic et al. 2000, Ryzhkov et al. 2007, Tabary et al. 2009a, Tabary et al. 2010) that the high Z_{dr} (3-8 dB) signature exists due to melting, resonant-sized, stably and horizontally oriented (i.e., with major axis in the horizontal) hailstones and large raindrops that are present at low-levels. The vertical profile of ρ_{hv} confirms this hypothesis by showing clear lowering below the height of the 0 °C level. Additionally, the environmental parameters presented in Table 2 show that melting hail is most likely present for each of these events near the surface. The clear lowering in ρ_{hv} (< 0.95) associated with resonance has been shown in the studies above to cause enhanced Z_{dr} (3 - 8 dB) for wet particles over 5 mm. In addition, melting may play a role in setting up the right conditions for resonance including the necessary size, shape, fall mode, and dielectric constant.

By comparing collocated S-band (insignificantly attenuated) to C-band (potentially highly attenuated) frequency radar observations, Borowska et al. (2011) demonstrate that in the case of strong hail bearing storms, phase-based propagation correction methods that estimate

mean corrections coefficients over the entire storm path, such as the Bringi et al. (2001) attenuation correction algorithm used herein, can under estimate the attenuation and differential attenuation in and beyond "hot spots" associated with melting hail and large rain drops. If this is the case, then even higher Z_h and Z_{dr} would be expected in and down range of hail producing regions or hot spots. In other words, the fundamental conclusion of this study would likely not change even if the enhanced propagation effects of these hot spots were individually addressed – i.e., melting hail near the surface at C-band is typically characterized by high Z_h (> 50 dBZ), high Z_{dr} (3 – 8 dB or more), and low ρ_{hv} (< 0.95). Nonetheless, more research is required to test the proposed operational propagation correction methods of Tabary et al. (2009b) and Gu et al. (2011), which deal specifically with hot spots at C-band, and verify the results of this study. Additionally, more C-band radar observations in a variety of meteorological environments along with thorough in-situ hydrometeor documentation, as begun in Tabary et al. (2009a) and (2010), are required to refine and confirm these results.

Acknowledgments. This work was funded by NOAA Grant NA09OAR4600204 in support of the UAHuntsville Tornado Hurricane and Observations Research Center (THOR). WAP and LDC also acknowledge support of the NASA Precipitation Science Program. The authors also acknowledge Patrick Gatlin of UAHuntsville for his assistance with ARMOR radar data and analysis.

REFERENCES

Aydin, K. T., T. Seliga, and V. Balaji, 1986: Remote sensing of hail with dual linear polarization radar. *J. Climate Appl. Meteor.*, **25**, 1475-1484.

Aydin, K., Zhao, Y., and Seliga, T. A., 1990: A differential reflectivity radar hail measurement technique: Observations during the Denver hailstorm of 13 June 1984. *J. Atmos. and Oceanic Tech.*, **7**, 104-113.

Aydin, K. and V. Giridhar, 1992: C-Band dual polarization radar observable in rain. *J. Atmos. Oceanic Technol.*, **9**, 383-390.

Balakrishnan N. and D. S. Zrnic 1990: Use of polarization to characterize precipitation and Discriminate large hail. *J. Atmos. Sci.*, **47**, 1525-1540.

Borowska, L., A. Ryzhkov, D. Zrnic, C. Simmer, and R. Palmer, 2011: Attenuation and differential attenuation of 5-cm-wavelength radiation in melting hail. *J. Appl. Meteor. Climatol.*, **50**, 59-76.

Bringi, V. N., T. A. Seliga, and K. Aydin, 1984: Hail detection with a differential reflectivity radar. *Science*, **225**, 1145-1147.

Bringi, V. N., J. Vivekanandan, and J. D. Tuttle, 1986: Multiparameter radar measurements in Colorado convective storms. Part II: Hail detection studies. *J. Atmos. Sci.*, **43**, 2564-2577.

Bringi, V. N., V. Chandrasekar, P. Meischner, J. Hubbert, and Y. Golestani, 1991: Polarimetric radar signatures of precipitation at S- and C-bands. *IEEE Trans. Remote Sens.*, **138**, 109-119.

Bringi, V. N., T. D. Keenan, V. Chandrasekar, 2001: Correcting C-Band Radar Reflectivity and differential reflectivity data for rain attenuation: a self-consistent method with constraints. *IEEE Trans. Remote Sens.*, **39**, 1906-1915.

Bringi, V. N. and V. Chandrasekar, 2001: Polarimetric Doppler weather radar: principles and applications. Cambridge University Press, Cambridge, 636 pp.

Carey, L. D., S. A. Rutledge, D. A. Ahijevych, and T. D. Keenan, 2000: Correcting propagation effects in C-band polarimetric radar observations of tropical convection using differential propagation phase. *J. Appl. Meteor.*, **39**, 1405-1433.

Changnon, S. A., 1999: Data and approaches for determining hail risk in the contiguous United States. *J. Appl. Meteor.*, **38**, 1730-1739.

Deierling, W., J. Latham, W. A. Petersen, J. Latham, S. Ellis, and H. J. Christian, 2008: The relationship between lightning activity and ice fluxes in thunderstorms. *J. Geophys. Res.*, **113**, D15210.

Depue, T. K., P. C. Kennedy, and S. A. Rutledge, 2007: Performance of the hail differential reflectivity (H_{DR}) polarimetric radar hail indicator. *J. Appl. Meteor. Clim.*, **46**, 1290-1301.

Dolan, B. and S. A. Rutledge, 2009: A theory-based hydrometeor identification algorithm for X-band polarimetric radars. *J. Atmos. Oceanic Technol.*, **26**, 2071-2088.

Eccles, P. J. and D. Atlas, 1973: A dual-wavelength hail detector. *J. Appl. Meteor.*, **5**, 847-854.

Edwards, R. and R. L. Thompson, 1998: Nationwide comparisons of hail size with WSR-88D vertically liquid integrated water and derived thermodynamic sounding data. *Wea. Forecasting*, **13**, 277-285.

Gorgucci, E., G. Scarchilli, and V. Chandrasekar, 1999: A procedure to calibrate multiparameter weather radar using properties of the rain medium. *IEEE Trans. Geosci. Remote Sens.*, **37**, 269-276.

Greene, D.R. and R. A. Clark, 1972: Vertically integrated liquid water-a new analysis tool. *Mon. Wea. Rev.*, **100**, 548-552.

Gu, J.-Y., A. Ryzhkov, P. Zhang, P. Neilley, M. Knight, B. Wolf, and D.-I., Lee, 2011: Polarimetric attenuation correction in heavy rain at C band. *J. Appl. Meteor. Climatol.*, **50**, 39-58.

Heinselman, P. L., and A. V. Ryzhkov, 2006: Validation of polarimetric hail detection. *Wea. Forecasting*, **21**, 839-850.

Herzegh, P. H. and A. R. Jameson, 1992: Observing precipitation through dual-polarization measurements. *Bull. Amer. Meteor. Soc.*, **73**, 1365-1374.

Hillaker, H. J. and P. J. Waite, 1985: Crop-hail damage in the Midwest corn belt. *J. Climate Appl. Meteor.*, **24**, 3-15.

Höller, H., V. N. Bringi, J. Hubbert, M. Hagen, and P. F. Meischner, 1994: Life cycle and precipitation formation in a hybrid-type hailstorm revealed by polarimetric and Doppler radar measurements. *J. Atmos. Sci.*, **51**, 2500-2522.

Hubbert, J., V. N. Bringi, L. D. Carey, and S. Bolen, 1998: CSU-CHILL polarimetric radar measurements from a severe hail storm in eastern Colorado. *J. Atmos. Sci.*, 749-775.

Illingworth, A. J., J. W. F. Goddard, and S. M. Cherry, 1986: Detection of hail by dual-polarization radar. Nature, **320**, 431-433.

Keenan, T. D., L. D. Carey, D. S. Zrnic, and P. T. May, 2000: Sensitivity of 5-cm wavelength polarimetric radar variables to raindrop axial ratio and drop size distribution. *J. Appl. Meteor.*, **40**, 526-545.

Keenan, T. D., 2003: Hydrometeor classification with a C-Band polarimetric radar. *Aust. Meteor. Mag.*, **52**, 23-31.

Leitao, M. J., and P. A. Watson, 1984: Application of dual linearly polarized radar data to prediction of microwave path attenuation at 10-30 GHz. *Radio Sci.*, **19**, 209-221.

Ludlam, F. H., 1980: Clouds and Storms: The Behavior and Effect of Water in the Atmosphere. The Pennsylvania State University Press, 405 pp.

Mather, G. K., D. Treddenick, and R. Parson, 1976: An observed relationship between the height of 45-dBZ contours in storm profile and surface hail reports. *J. Appl. Meteor.*, **15**, 1336-1340.

Meischner P. F., V. N. Bringi, D. Heimann, and H. Höller, 1991: A squall line in southern Germany: kinematics and precipitation formation as deduced by advanced polarimetric and Doppler radar measurements. *Mon. Wea. Rev.*, **119**, 678-701.

Petersen, W. A., K. R. Knupp, D. J. Cecil, and J. R. Mecikalski, 2007: The University of Alabama Huntsville THOR Center instrumentation: Research and operational collaboration. 33rd International Conference on Radar Meteorology, American Meteorological Society, Cairns, Australia, August 6-10, 2007.

Rasmussen, R. M., and A. J. Heymsfield, 1987a: Melting and shedding of graupel and hail. Part I: Model physics. *J. Atmos. Sci.*, **44**, 2754-2763.

Rasmussen, R. M., and A. J. Heymsfield, 1987b: Melting and shedding of graupel and hail. Part II: Sensitivity study. *J. Atmos. Sci.*, **44**, 2764-2782.

Rasmussen, R. M., and H. R. Pruppacher, 1982: A wind tunnel and theoretical study of the melting behavior of atmospheric ice particles. I: A wind tunnel study of frozen drops of radius < 500 μm. *J. Atmos. Sci.*, **39**, 152-158.

Ryzhkov, A. V., S. E. Giangrande, V. M. Melnikov, and T. J. Schuur, 2005: Calibration issues of dual polarization radar measurements. *J. Atmos. Oceanic Technol.*, **22**, 1138-1155.

Ryzhkov, A. V., D. S. Zrnic, P. Zhang J. Krause, H. S. Park, D. Hudak. J. Young, J. L. Alford, M. Knight, and J. W. Conway, 2007: Comparison of polarimetric algorithms for hydrometeor classification at S and C bands, *33rd Conference on Radar Meteorology*, Caims, Queensland, 5-10, August 2007.

Ryzhkov, A. V.: Polarimetric characteristics of melting hail at S and C bands, 2009: *34th Conference on Radar Meteorology*, Williamsburg, VA, 5-9, October 2009.

Snyder, J. C., H. B. Bluestein, G. Zhang, S. J. Frasier, 2010: Attenuation correction and Hydrometeor classification of high-resolution, X-band, dual-polarized mobile radar measurements in severe convective storms. *J. Atmos. Oceanic Technol.*, **27**, 1979-2001.

Straka, J. M., D. S. Zrnic, and A. V. Ryzhkov, 2000: Bulk hydrometeor classification and quantification using polarimetric radar data: synthesis of relations. *J. Appl. Meteor.*, **39**, 1341-1372.

Tabary, P., B. Fradon, A. J. Illingworth, and G. Vulpiani, 2009a: Hail detection and quantification with a C-band polarimetric radar: Challenges and promises. *34th Conference on Radar Meteorology*, Williamsburg, VA, 5-9, October 2009.

Tabary, P., F. Vulpiani, J. J. Gourley, A. J. Illingworth, R. J. Thompson, and O. Bousquet, 2009b: Unusually high differential attenuation at C-band: Results from a two-year

analysis of the French Trappes polarimetric radar data. *J. Appl. Meteor. Clim.*, **48**, 2037-2053.

Tabary, P., C. Berthet, P. Dupuy, J. Figueras, B. Fradon, J. F. Georgis, R. Hogan, F. Kabeche, and J. P. Wasselin, 2010: Hail detection and quantification with C-band polarimetric radars: Results from a two-year objective comparison against hailpads in the south of France, *6th ERAD*, Sibiu, Romania, 6-10, September 2010.

Vivekanandan, J., V. N. Bringi, and R. Raghavan, 1990: Multiparameter radar modeling and observations of melting ice. *J. Atmos. Sci.*, **47**, 549-564.

Wakimoto, R. M. and V. N. Bringi, 1988: Dual-polarization observations of microburst associated with intense convection: The 20 July storm during the MIST project. *Mon. Wea. Rev.*, **116**, 1521-1539.

Yuter, S. A. and R. A. Houze, 1995: Three-dimensional kinematics and microphysical evolution of Florida cumulonimbus. Part II: Frequency distribution of vertical velocity , reflectivity, and differential reflectivity. *Mon. Wea. Rev.*, **123**, 1941-1963.

Zrnic, D. S., T. D. Keenan, L. D. Carey, P. May, 2000: Sensitivity analysis of polarimetric variables at a 5-cm wavelength radar in rain. *J. Appl. Meteor.*, **39**, 1514-1526.

TABLES AND FIGURES

Table 1. Overview of Hail Events

Date	*Number of Cells*	*Number of Hail Reports*	*Average Hail Size*	*Hail Size Range (Minimum to Maximum)*
February 21, 2005	9	25	2.4 cm	1.9 – 4.5 cm
April 3, 2007	2	9	2.4 cm	1.9 – 4.5 cm
March 15, 2008	4	7	2.1 cm	1.9 – 2.2 cm
August 2, 2008	4	19	3.3 cm	1.9 – 4.5 cm
March 28, 2009	4	4	2.5 cm	1.9 – 3.2 cm
April 10, 2009	5	77	4.0 cm	0.6 – 10.8 cm
April 13, 2009	3	4	2.3 cm	1.9 – 2.5 cm
January 21, 2010	2	6	3.3 cm	1.3 – 7.0 cm
March 12, 2010	10	21	2.9 cm	1.9 – 4.5 cm
Total:	46	172	3.3 cm	0.6 – 10.8 cm

Table 2. Overview of Environmental Parameters

Date	*Height of 0 °C*	*Lapse Rate (700-500 mb)*	*Average Mid-Level RH (700-500 mb)*	Surface Temperature
February 21, 2005	3.17 km	6.0 °C/km	43 %	21.1 °C
April 3, 2007	3.70 km	6.8 °C/km	33 %	26.4 °C
March 15, 2008	3.21 km	7.4 °C/km	30%	17.2 °C
August 2, 2008	4.81 km	6.3 °C/km	49 %	30.9 °C
March 28, 2009	3.22 km	5.5 °C/km	65 %	21.2 °C
April 10, 2009	2.99 km	7.6 °C/km	14 %	21.2 °C
April 13, 2009	2.81 km	5.1 °C/km	74 %	20.9 °C
January 21, 2010	2.64 km	6.8 °C/km	76 %	18.5 °C
March 12, 2010	2.85 km	7.2 °C/km	86 %	14.1 °C
Average:	3.27 km	6.5 °C/km	52 %	21.3 °C

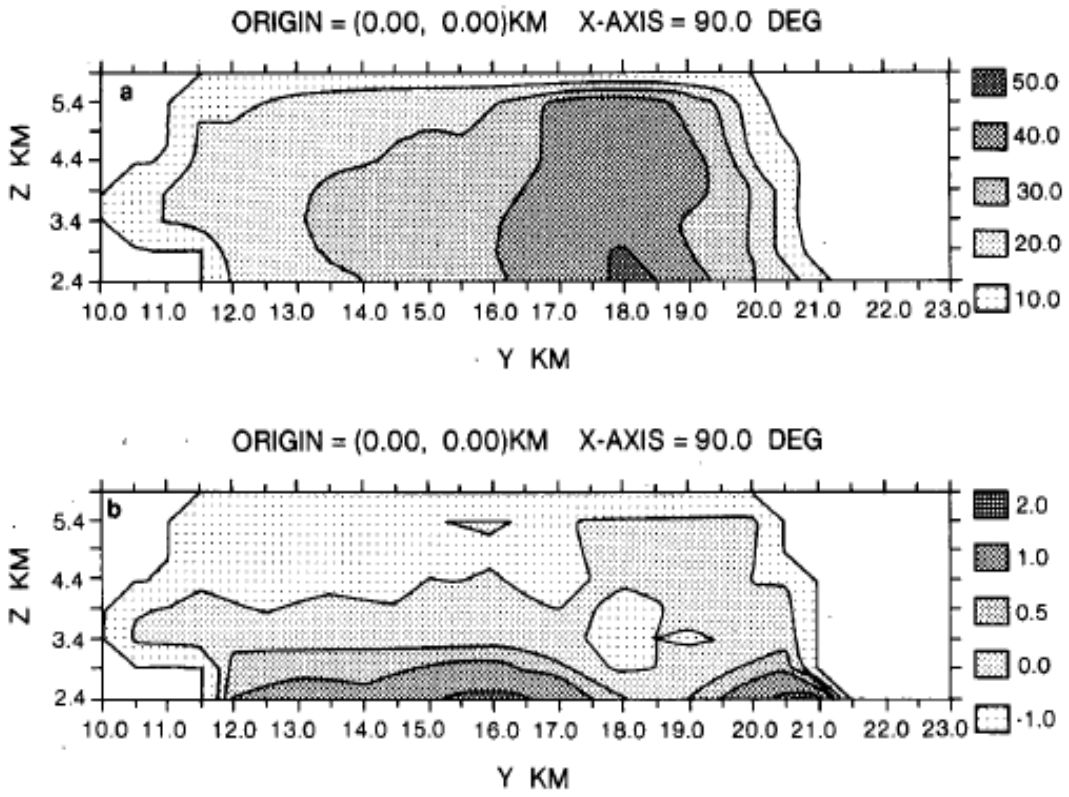

Figure 1. Adapted from Bringi et al. (1986). (a) Range Height Indicator (RHI) of reflectivity and (b) Z_{dr} in contours through a hail producing convective cell at S-band. The dual polarimetric radar-based hail signature, or "Z_{dr}-hole", is observed between 18 and 19 km. (c) American Meteorological Society. Reprinted with permission.

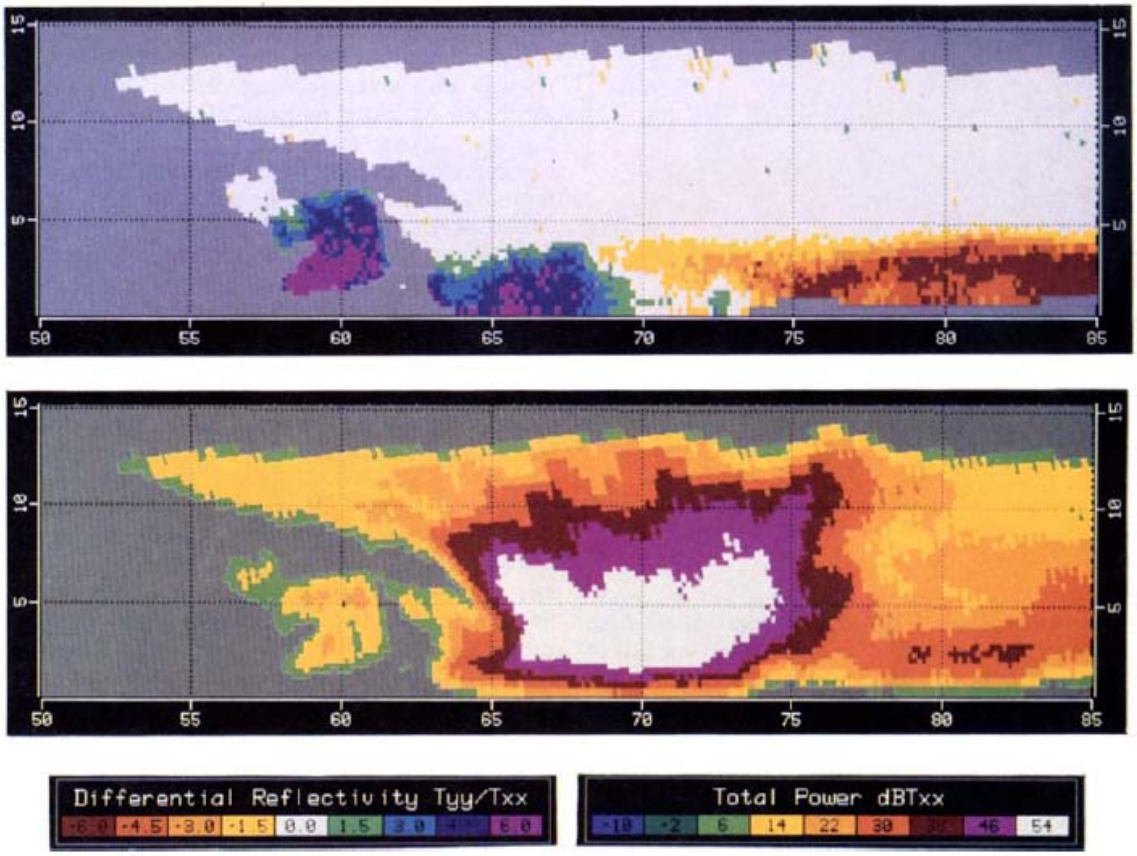

Figure 2. Adapted from Meischner et al. (1991). Vertical cross section (RHI) of Z_{dr} (top panel) and Z_h (bottom panel) through a hailstorm at C-band. High Z_{dr} (> 5 dB) associated with high Z_h (> 45 dBZ) can be seen between 65 and 70 km. (c) American Meteorological Society. Reprinted with permission.

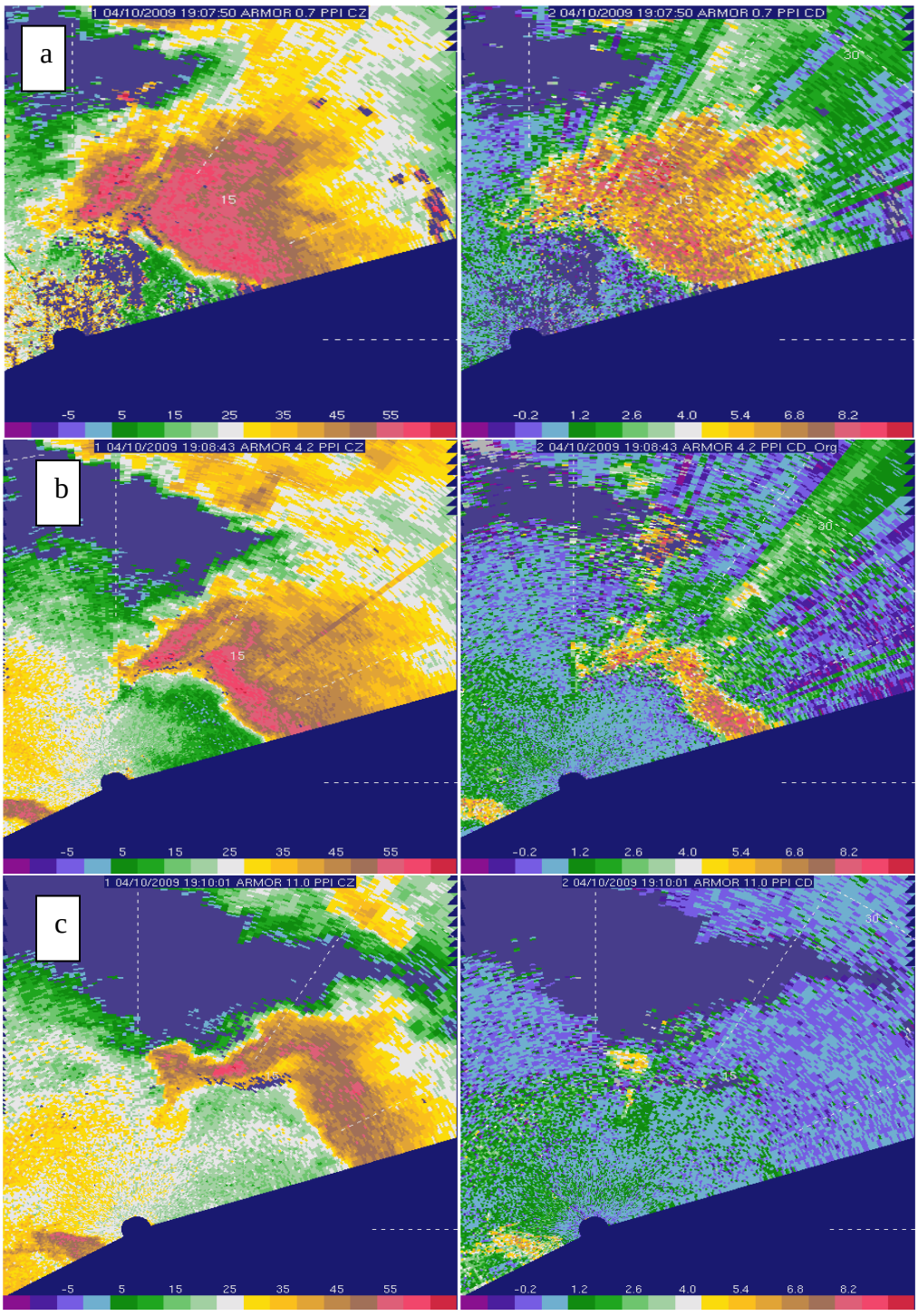

Figure 3. ARMOR Plan Position Indicator (PPI) view of Z_h (dBZ) (left) and Z_{dr} (dB) (right) on April 10, 2009 at 1907 UTC at (a) 0.7°, (b) 4.2°, and (c) 11.0° elevation angles. Horizontal east-west distance from ARMOR (km) versus north-south distance from ARMOR is shown.

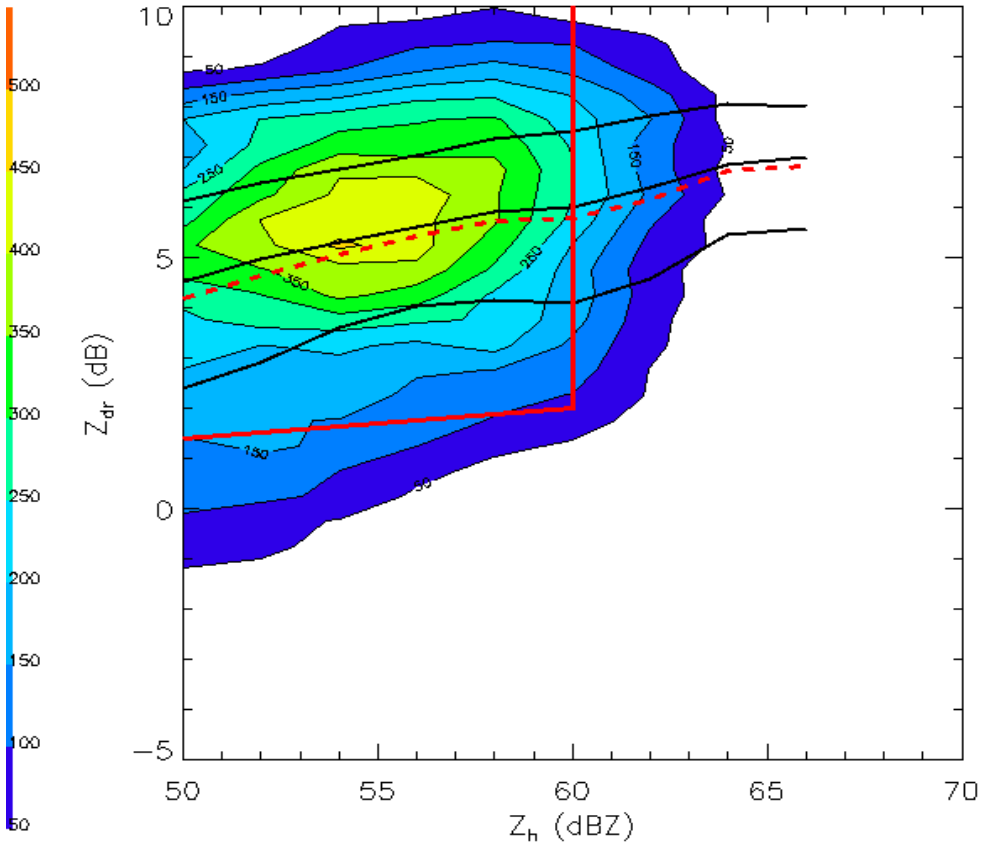

Figure 4. Joint frequency histogram of ARMOR Z_{dr} versus Z_h at low levels for April 10, 2009. All ARMOR data are taken from the lowest 1 km in height above the surface and from within 1 km horizontal distance of a hail report for values of Z_h > 45 dBZ. The Z_h data are in 2 dB bins and the Z_{dr} data are in 0.5 dB bins. The thick black lines from bottom to top are the 25th, 50th, and 75th percentiles. The dashed red line is the mean. The solid red line is where H_{dr} = 0 dB.

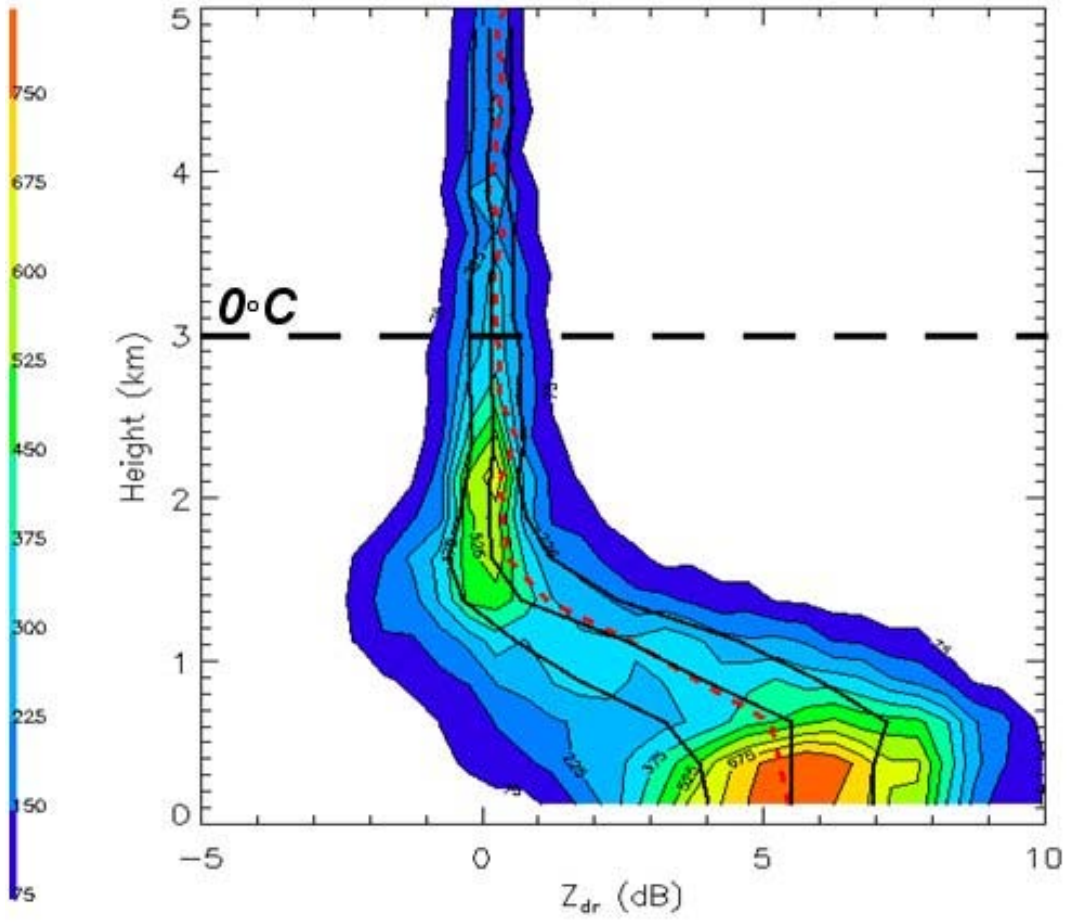

Figure 5. Contoured frequency by altitude diagram (CFAD) of Z_{dr} for the April 10, 2009 ARMOR data set. All data are located within 1 km of a hail report from the April 10, 2009 data set for values of Z_h > 45 dBZ. The Z_{dr} data are in 0.5 dB bins and the height data are in 250 m bins. The thick black lines from left to right are the 25th, 50th, and 75th percentiles. The red dashed line is the mean. The height of the 0° C level is indicated (3.0 km).

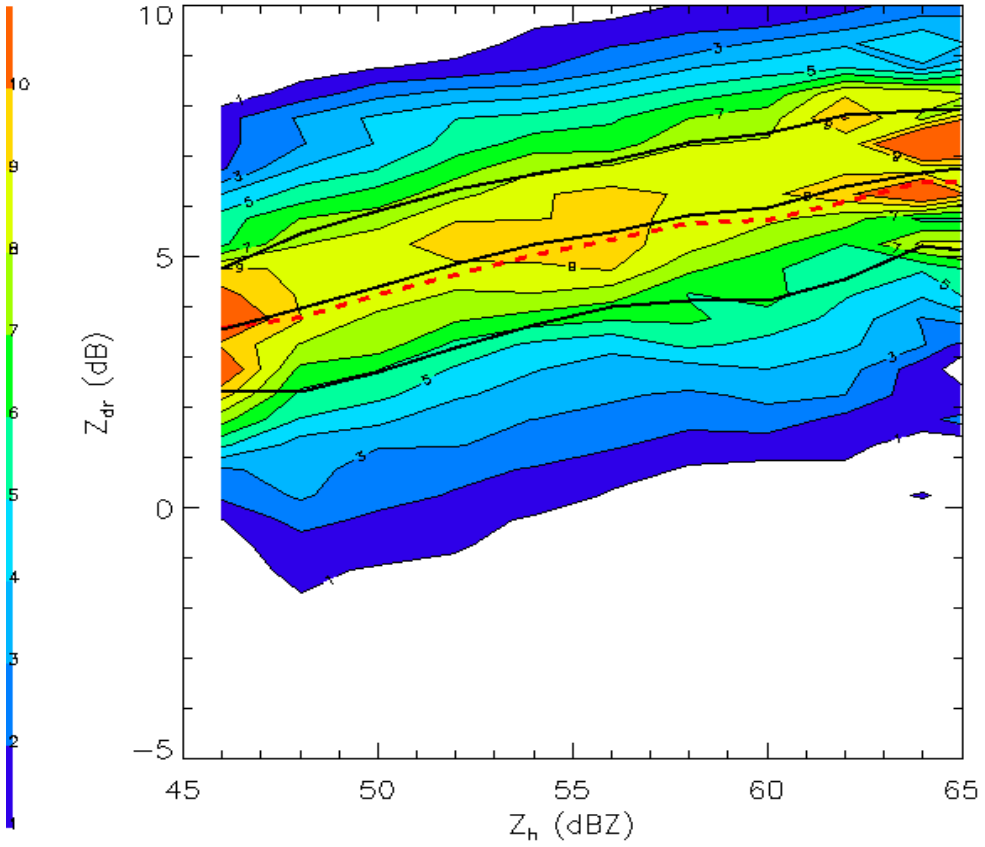

Figure 6. Composite joint relative frequency histogram in percent of ARMOR Z_{dr} versus Z_h at low levels for all hail events in Table 1. All data are taken from the lowest 1 km in height above the surface and from within 1 km horizontal distance of a hail report from the composite data set of all nine events for values of Z_h > 45 dBZ. The Z_h data are in 2 dB bins and the Z_{dr} data are in 0.5 dB bins. The thick black lines from bottom to top are the 25th, 50th, and 75th percentiles. The dashed red line is the mean.

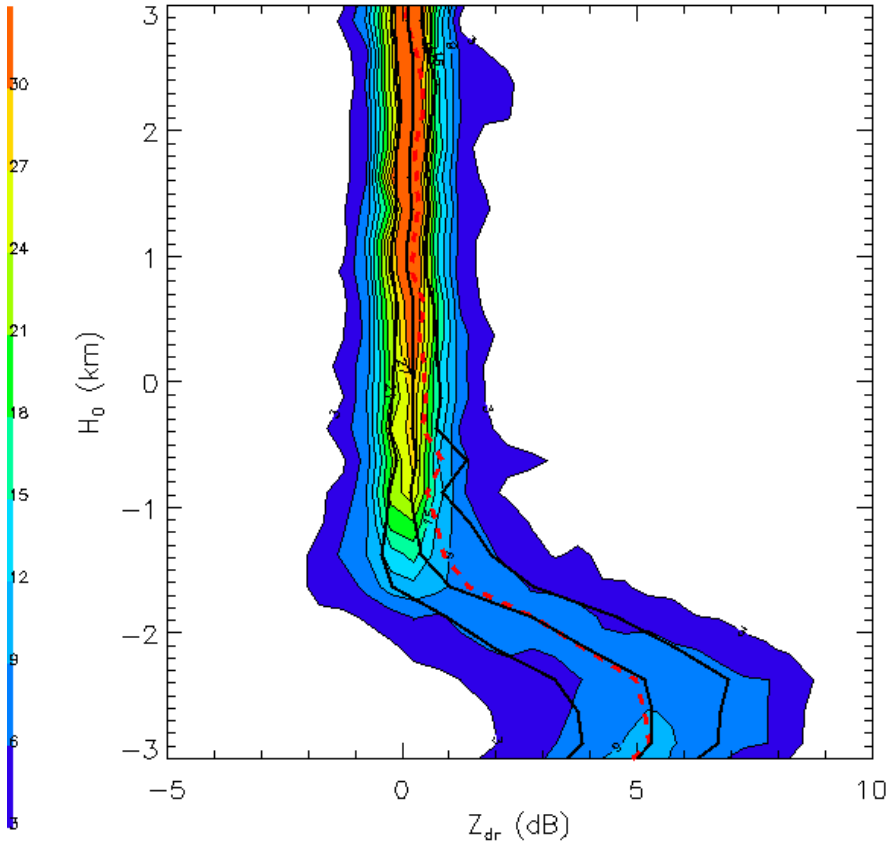

Figure 7. Contoured frequency by altitude diagram (CFAD) expressed in percent of ARMOR Z_{dr} (dB) versus height relative to the 0 °C level (H_0, km) for all hail events in Table 1. All data are located within 1 km of a hail report from the composite data set from nine events for values of Z_h > 45 dBZ. The Z_{dr} data are in 2 dB bins and the height data are in 250 m bins. The thick black lines from left to right are the 25th, 50th, and 75th percentiles. The red dashed line is the mean.

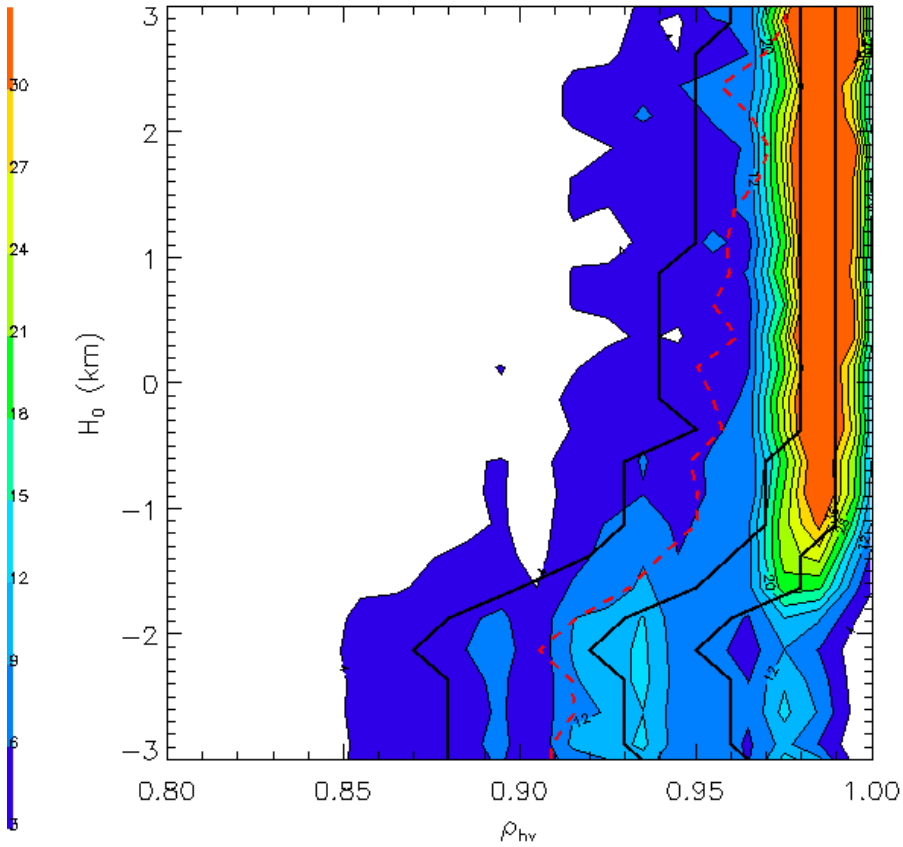

Figure 8. Contoured frequency by altitude diagram (CFAD) expressed in percent of ARMOR ρ_{hv} versus height relative to the 0 °C level (H_0, km) for all hail events in Table 1. All data are located within 1 km of a hail report from the composite data set from nine events for values of Z_h > 45 dBZ. The ρ_{hv} data are in 0.01 bins and the height data are in 250 m bins. The thick black lines from left to right are the 25th, 50th, and 75th percentiles. The red dashed line is the mean.